

# Spectral Spaces and Color Spaces

Rajeev Ramanath,<sup>1\*</sup> Rolf G. Kuehni,<sup>2</sup>  
Wesley E. Snyder,<sup>1</sup> David Hinks<sup>2</sup>

<sup>1</sup> Department of Electrical and Computer Engineering, North Carolina State University, Raleigh, NC

<sup>2</sup> Department of Textiles Engineering, Chemistry and Science, North Carolina State University, Raleigh, NC

Received 17 June 2002; revised 25 October 2002; accepted 13 January 2003

*It has long been known that color experiences under controlled conditions may be ordered into a color space based on three primary attributes. It is also known that the color of an object depends on its spectral reflectance function, among other factors. Using dimensionality reduction techniques applied to reflectance measurements (in our case a published set of 1 nm interval reflectance functions of Munsell color chips) it is possible to construct 3D spaces of various kinds. In this article we compare color spaces, perceptual or based on dimensionality reduction using color matching functions and additional operations (uniform color space), to spectral spaces derived with a variety of dimensionality reduction techniques. Most spectral spaces put object spectra into the ordinal order of a psychological color space, but so do many random continuous functions. In terms of interval scales there are large differences between color and spectral spaces. In spectral spaces psychophysical metamers are located in different places.*

© 2003 Wiley Periodicals, Inc. *Col Res Appl*, 29, 29–37, 2004; Published online in Wiley InterScience (www.interscience.wiley.com). DOI 10.1002/col.10211

*Key words:* color spaces; metamerism; Munsell system; spectral spaces; spectrophotometry

## INTRODUCTION

In recent years interest in spectral spaces representing in a limited number of dimensions (usually three) the reflectances of color chips defining perceptual color spaces [those of Munsell or Swedish Natural Color System (NCS)] and

other data has increased.<sup>1–6</sup> Different mathematical techniques have been used for the dimensionality reduction with varying results.

Color spaces are usually defined as geometrical models of human color experiences. Perceptual color spaces are geometrical arrangements of color chips (or geometrical models thereof) found under given conditions to differ from each other in specific ways. In the case of the Munsell system, for example, the color chips differ in terms of the color attributes hue, chroma (saturation) and value (lightness) by unit differences that vary by attribute. In the case of NCS they vary by unique hue component, blackness and whiteness.

Psychophysical color spaces are based on the weighting of the spectral return (the products of a normalized spectral power function defining the light source and the spectral reflectance function of the objects viewed) entering the eye that views samples in a given surround by cone response or color matching functions, and additional manipulation. These spaces assume the premise that there is a direct and unique relationship between the spectral return entering the eye and the resulting color experience. At least since Land's experiments it is known that this premise is not generally valid because a given spectral return can result in widely differing color experiences depending on the complexity of the surround. Reasonably good correlation between spectral return and experience can be obtained when maximally simplifying the surround to a single, uniform achromatic field.

There is a fundamental difference between spectral spaces and color spaces, the former being based on implicit weighting by functions derived from mathematical analysis of spectral returns, the latter on the explicit weighting by functions based on results of color-matching experiments, i.e., psychological data. The purpose of this article is to compare the two kinds of spaces and to demonstrate the

\* Correspondence to: Rajeev Ramanath, Department of Electrical and Computer Engineering, North Carolina State University, Box 7911, Raleigh, NC 27695-7914 (e-mail: rajeev.ramanath@ieee.org)  
© 2003 Wiley Periodicals, Inc.

differences that are critical from the point of view of color vision.

## BACKGROUND

Historically, psychological color spaces are geometrical Euclidean three-dimensional (3D) arrangements of color chips that vary in a given perceptual fashion. A Euclidean arrangement is only possible if the unit differences of the different attributes used for the arrangement are not of equal size. In the Munsell system, for example, the scale units of hue, value and chroma scales are all of different perceptual size. For the last 100 years the most sought after color space has been the perceptually uniform one, with no fully satisfactory solution as yet. Another well-known space is based on constant change in perceived unique hues, blackness and whiteness (the so-called Hering natural color space). In terms of perceptual distance this space varies between and within attributes.

### Psychophysical Color Spaces

Psychophysical color spaces are based on spectral returns and cone sensitivity or color-matching functions. In human color vision the spectral returns are subject, among other things, to lightness and chromatic adaptation effects. These tend to discount, to a smaller or larger extent, the effect of the spectral composition of the light source. It is reasonable to assume that adaptation to a (synthetic) equal energy light source would lead to color experiences very similar to those of, say, daylight illuminant D55 and that as a first approximation an average daylight source can be discounted and spectral returns (on a relative basis) can be considered to be the spectral reflectance functions.

The colorimetric system reduces the many dimensions (typically 31 at 10 nm intervals) of spectral returns to three by subjecting them to the filters or weights of the standardized color-matching functions. Color matching bears some relationship to color appearance since matched lights or objects have the same appearance. However, matching does not provide explicit information about the relationship between reflectance function and appearance (in the highly relativized condition where a systematic relationship can be expected). When placing Munsell system reflectance functions into the CIE tristimulus space they form an irregular, slanted double cone, with the perfect black color at the origin of the space. Planes of constant value are horizontal slices through the slanted double cone. In order to make the lightness axis perpendicular to the constant value planes, the additional assumption of an operating opponent color system is made. This is achieved by normalizing by subtracting (and application of a weighting factor) the  $X$  and  $Z$  tristimulus values from  $Y$ . A plane chromatic diagram results in which perfectly horizontal reflectance functions under an equal energy light source, regardless of their luminous reflectance, fall on the origin. Fair agreement with the psychological space is still not obtained because the (relativized) relationship between reflectance function and color

experience is not linear. Appropriate power functions applied to the tristimulus values or the opponent color values improve the agreement considerably. If the filters used are cone-response functions rather than color-matching functions an additional transformation is required to convert the former to the latter (or approximations thereof).

The several steps discussed generate points in a 3D space from reflectance functions, the distribution of which indicates a degree of agreement with the distribution of points representing, say, Munsell chips in a psychologically derived hue, value, chroma space.

### Spectral Spaces

Reflectance functions can be weighted or filtered by many functions other than cone response or color matching functions. Of particular interest in recent years have been functions that represent the information content in reflectance functions more completely than color matching functions. They allow reconstruction of the original reflectance functions with a good to high degree of accuracy, depending on the number of functions. In case of three functions they can be interpreted as axial definitions of a space. Spectral spaces and color spaces are therefore, alternative methods to reduce the dimensionality of spectral data.

## DIMENSIONALITY REDUCTION TECHNIQUES (NON-PSYCHOPHYSICAL)

Cohen was the first to make use of dimensionality reduction techniques as a mathematical tool to analyze reflectance spectra.<sup>1</sup> Many researchers since have sought to find what may be called the “best” space representation of measured spectral reflectance functions. Such techniques may be broadly classified either as having non-negative bases (all-positive or AP) or as having a mixture of positive and positive-negative bases (PN).<sup>a</sup>

### Spaces Described by PN Bases

Within PN-type spaces, the most popular technique is Principal Component Analysis (PCA).<sup>7-9</sup> It has basis functions that correspond to directions having maximum variance, the idea being that the direction(s) in which the measured data has most variance is accounted for. The use of PCA inherently implies that we are forcing a Gaussian form on the distribution of the data. This need not always be true. Given a set of  $N$  reflectance measurements  $x_i \in \mathfrak{R}^M$  (each of the  $N$  reflectance functions has  $M$  samples), stacked into an  $M \times N$  matrix  $X$ , we can construct an  $M \times M$  matrix  $E = XX^T$ . This matrix is non-singular and all non-zero scalars  $\lambda$  and non-zero vectors  $\bar{y}$  satisfying  $E \cdot \bar{y} = \lambda \cdot \bar{y}$  are called *eigenvalues* and *eigenvectors* respectively, and any such pair  $(\lambda, \bar{y})$  is called an *eigenpair*. For the purposes of our

<sup>a</sup> These techniques are only briefly discussed; the reader interested in more details is referred to the references.

experiment, we shall deal with the eigenpairs corresponding to the three largest eigenvalues.

Independent Component Analysis (ICA) is another technique for dimensionality reduction. It produces basis functions that give rise to maximum statistical independence of the data.<sup>10</sup> ICA represents an attempt at maximizing the non-Gaussian nature of the projected data, the result need not be bases that are orthogonal to each other. Laamanen *et al.* used ICA for dimensionality reduction of the Munsell spectral reflectance space.<sup>11</sup> These authors however did not provide a comparison of ICA with other techniques in the reduced dimensionality space. ICA is a product of research in signal processing in an effort to perform signal separation and source localization. A measured spectrum  $x_i \in \mathfrak{R}^M$  may be considered as a signal arising from linear combinations of signals from three (or more) sources  $s_j \in \mathfrak{R}^M$ ,  $j = 1, 2, 3 \dots J$ . In case of three sources this is given by  $x_i = a_{i1}s_1 + a_{i2}s_2 + a_{i3}s_3$ . This set of linear combinations may be represented in matrix notation by  $X = AS$ , where  $A$  is called the mixing matrix and is composed of rows, each representing the weights used to construct  $x_i$  from the various independent components (ICs) $s_j$ ,  $S$  is a matrix formed by stacking the various  $s_j$  values as its columns and  $X$  is a matrix whose columns represent the  $N$  different measured reflectances. The objective of ICA is to find the entries in  $A$  and also solve for such that the  $s_j$  functions are statistically independent of each other. A fuller description of ICA may be found in references 10 and 11.

Neural networks (NN) have been known to “learn” certain properties of data presented to it and are able to perform well with “unseen” data. The network does not make assumptions about the distribution of the data. A popular version of NN used for dimensionality reduction is an auto-encoder that has a decreasing number of neurons in each layer. Usui *et al.* first used a NN for dimensionality reduction of the reflectance spectra of Munsell color chips.<sup>12</sup> Such a NN is a combination of an auto-encoder and a decoder.<sup>13</sup> Neural networks require a significant amount of time for learning the structure of the data, but once trained the network performs with a speed comparable to that of other methods. The basis functions of neural networks cannot be “plotted” (they cannot be “tracked” through multiple layers). The weights of the neurons are representative of the basis functions and have both positive and negative values.

### Space Described by AP Bases

The color imaging industry has a need for non-negative basis functions.<sup>14</sup> Lee and Seung recently developed a matrix factorization technique called Non-negative Matrix Factorization (NMF)<sup>15</sup>. It extracts bases that have all positive entries. Buchsbaum and Bloch have used it for finding non-negative bases of the space containing the reflectance functions of Munsell color chips.<sup>16</sup> In NMF, just like in PCA and ICA, each measurement  $x_i \in \mathfrak{R}^M$  may be considered to be a weighted sum of three components. But, only

additive combinations are permitted. Using a notation similar to that used for describing ICA, consider reconstructions  $\hat{X} = AS$  of the original non-negative data  $X$  (the columns of which are the  $N$  different reflectance functions). Lee and Seung approach the problem of finding non-negative bases by assuming that the data is obtained from a Poisson distribution of mean  $AS$ .<sup>17</sup> Also assuming that the various data are statistically independent, the posterior distribution of obtaining  $X$  is given by  $p(X_{ij} | (AS)_{ij}) = \prod_i \prod_j \exp(-(AS)_{ij}) ((AS)_{ij})^{X_{ij}} / X_{ij}!$ , where  $i = 1, 2, 3 \dots M$  and  $j = 1, 2, 3 \dots N$ . Since the logarithm is a monotonic function, maximizing the above functional is the same as maximizing its logarithm. The objective function boils down to maximizing  $\sum_i \sum_j [-(AS)_{ij} + X_{ij} \ln(AS)_{ij} - \ln(X_{ij}!)]$ . With random initializations for the matrices  $A$  and  $S$  the above objective function is maximized iteratively with all positive constraints on the elements of  $A$  and  $S$ . Details of the procedure may be found in the article by Lee and Seung.<sup>15</sup>

### SPECTRAL DATABASE AND METHODOLOGY

The Munsell spectral database of 1269 samples has been used for the calculation of spectral dimensionality reduction functions. This database is available at the University of Joensuu ftp server located at <ftp://ftp.lut.fi/pub/color/spectra/mspec>. It represents spectral measurements at 1-nm intervals from 380 to 800 nm of all available chromatic Munsell color chips. It does not contain all colors of the Munsell Renotations.<sup>18</sup> In particular; it does not contain measurements of achromatic samples. Value 5 and 7 samples have been synthesized by using perfectly flat functions at the appropriate reflectance values.

There is a significant difference between the  $x$ ,  $y$ ,  $Y$  values of the Munsell Renotations and those calculated from the measured 1-nm interval reflectances. There are at least three reasons for the difference: 1. The samples used in the measurements of the Joensuu data are not in exact agreement with the aim values of the Munsell Renotations. 2. The spectral interval of measurement of color chips used in the definition of the Renotations is 10 nm and 1 nm for the Joensuu data. 3. The spectral range of the Joensuu data is extended to 800 nm at the long-wave end while it stops at 720 nm for the Munsell Renotations. To give an indication of the difference the average CIELAB total color difference between the Renotations and the Joensuu data, for an equal energy illuminant, have been calculated for the 58 samples of the Value 7 “Celtic cross” (see Fig. 6 for example). The average  $\Delta E_{ab}^*$  error is found to be 5.65 with a standard deviation of 1.95. Unlike the Munsell Renotations, the Joensuu hue circle samples do not have a smoothly rounded arrangement in  $X$ ,  $Y$ ,  $Z$  space and because of differences in luminous reflectance they do not fall exactly on a constant  $Y$  plane.

An equal energy light source was assumed for reasons given earlier. Calculations were performed on the original database with a range from 380–800 nm as well as on data where the spectral range has been reduced to 430–660 nm.

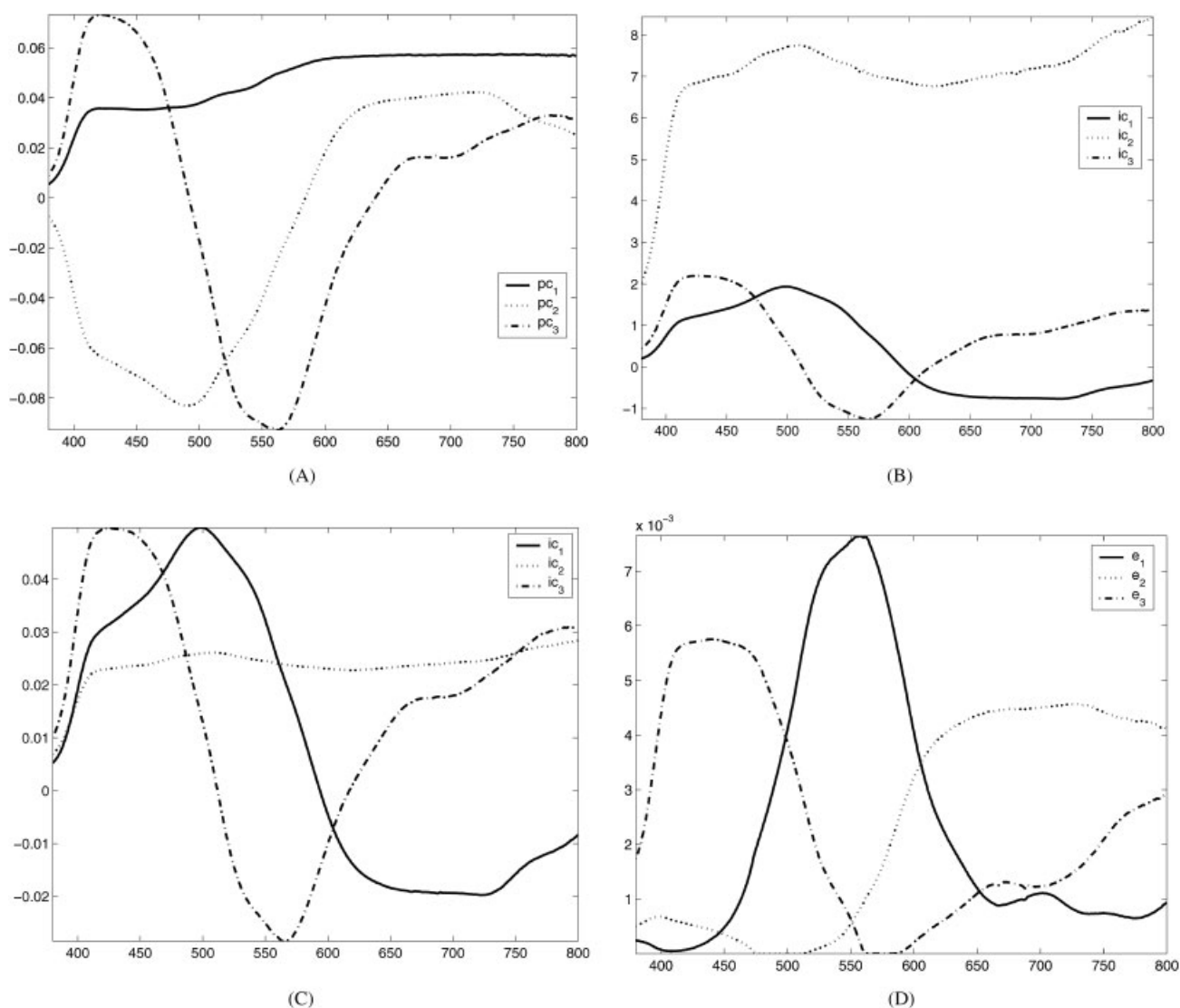


FIG. 1. Basis functions for the Munsell spectral database when using the wavelength range of 380–800nm (A) Eigen functions corresponding to the top three eigenvalues using PCA, (B) using ICA, (C) ICA bases, normalized to unit vectors; note similarity to PCA bases, (D) using NMF. Note that the basis vectors span the same space if the sign is reversed. Also note that with ICA, the sequence of the bases is irrelevant.

The latter reduced range better approximates the spectral sensitivities of the human visual system. A similarly reduced spectral range has recently been used by Romney and Indow.<sup>19</sup>

To be able to perform a comparison at comparable levels, we chose to use three bases for each of the dimensional reduction techniques. For PCA, the three largest eigenvectors were chosen as representative of the database. For ICA and NMF, the optimization for the choice of bases was performed for three vectors only. The neural network chosen is similar to that used by Usui *et al.*<sup>12</sup> It has a “wine-glass” structure, with neurons organized in 5 layers as 210-10-3-10-210 and 115-10-3-10-115 for the 380–800 nm and 430–660 nm cases, respectively. A gradient descent minimization was used with 0.01 as the stopping criterion (the value of the error function, the mean squared sum of the difference between the input and the estimated output).

## RESULTS AND DISCUSSION

### Comparison of Basis Functions

The basis functions obtained by applying different dimensionality reduction techniques for the spectral range 380–800 nm are shown in Fig. 1. The independent components of the ICA analysis are very similar to the eigenvectors of the PCA analysis. The visual difference is caused by the fact that the functions have not been normalized. In other words, the resulting 3D spaces are very similar and so are the basis functions (when normalized to unit vectors).

Figure 2 illustrates the basis function of the 430–660 nm spectral range for ICA. They are considerably different from those obtained for the 380–800 nm range, i.e., the two corresponding spaces differ as a function of the spectral range. As shown by Laamanen, Jaaskelainen and Parkkinen,

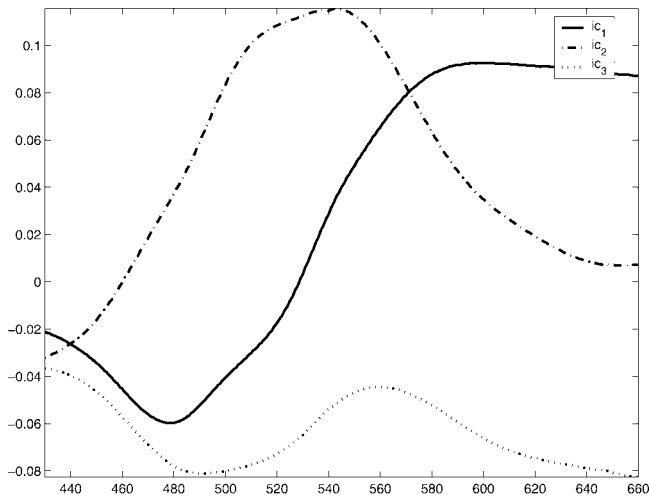


FIG. 2. Basis functions for the Munsell spectral database when using the wavelength range 430–660 nm using ICA.

principal spectral functions depend on the spectral data used to calculate them. Thus, from separate sets of visual metamers or from the Munsell and the NCS spectral data different functions are obtained.<sup>11</sup>

#### Accuracy of Reconstructed Reflectance Functions

The performance of the various dimensionality reduction techniques in reconstructing the reflectance functions in the two spectral ranges is listed in Table I. The neural network has been trained until a very small error was reached. Comparing the performance of the other systems to NN based upon these measures alone is, therefore not appropriate. We shall address this issue later. In the table the reconstruction accuracy is also shown for color matching functions (identical results are obtained for cone sensitivity as well as opponent functions linearly derived from the color matching functions).

It can be seen from the measures in Table I that three-dimensional PCA, ICA and NMF perform well in their abilities to reproduce the spectra of the samples. In case of PCA, ICA and NMF the accuracy can be improved by using more than three dimensions. The estimation of the reflectance functions from the three-dimensional values was done using a pseudoinverse algorithm without any constraints on the matrices involved. In other words, assuming that the  $M$  dimensional samples are encoded into 3D measurements us-

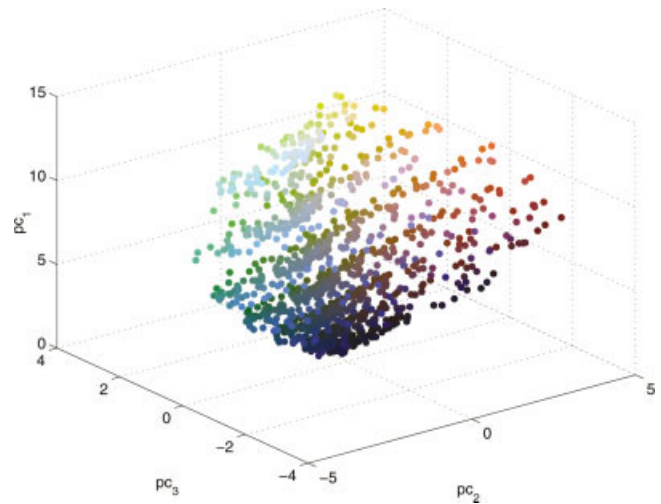


FIG. 3. Rendition of the 3D space resulting from a PCA-based dimensionality reduction.

ing a linear model  $Y = B^T X$ , where the rows of  $X$  contain the  $M$  spectral measurements and the various samples are stacked as columns;  $B$  is the transformation matrix and  $Y$  is the resulting 3D representation. The corresponding estimates of the reflectance functions are given by  $\hat{X} = (BB^T)^{-1}BY$ .

The poor performance of the 2 deg color-matching functions does not come as a surprise as the sensitivity functions are almost zero beyond the 700 nm wavelength, clearly not being able to reproduce non-zero reflectance functions beyond 700 nm. Considerable improvement is obtained for the narrow spectral range. However, the error is still significantly higher than that of the other weights. In addition, it is evident that the accuracy of all methods depends on the spectral range.

*Spaces of Munsell Data.* As an illustration of the structure of spectral spaces, we have included in Fig. 3, a 3D representation of all 1269 Munsell spectra in PCA. The color in this figure is not accurate and is provided as an orientation guide only. Animations of this and the NMF and ICA spaces may be found at <http://www.ece.ncsu.edu/imaging/Projects/SpectralSpaces>.

*Organization of Spectral and Psychophysical Color Spaces.* Like the cone response or the color matching functions PN and AP bases (with the exception of NN) place a Munsell hue circle, chroma and value scales in an order that is in ordinal agreement with the psychological order. (In NN

TABLE I. Error measures of the various reconstructions for the two wavelength ranges.

Method used		MSE	Max	Min	Variance	95th percentile
PCA	380–800 nm	0.3176	9.0823	0.0056	0.3098	1.0136
	430–660 nm	0.1071	2.3795	0.0005	0.0371	0.4324
ICA	380–800 nm	0.3581	9.2461	0.0113	0.3006	0.9324
	430–660 nm	0.9854	5.9959	0.0042	1.5119	3.5664
NMF	380–800 nm	0.3932	10.8585	0.0090	0.4442	1.1212
	430–660 nm	0.1257	2.5909	0.0002	0.0466	0.5568
CMFs	380–800 nm	25.8634	113.5626	0.4414	778.2233	86.5720
	430–660 nm	3.6709	16.6888	0.0507	15.1270	12.4693

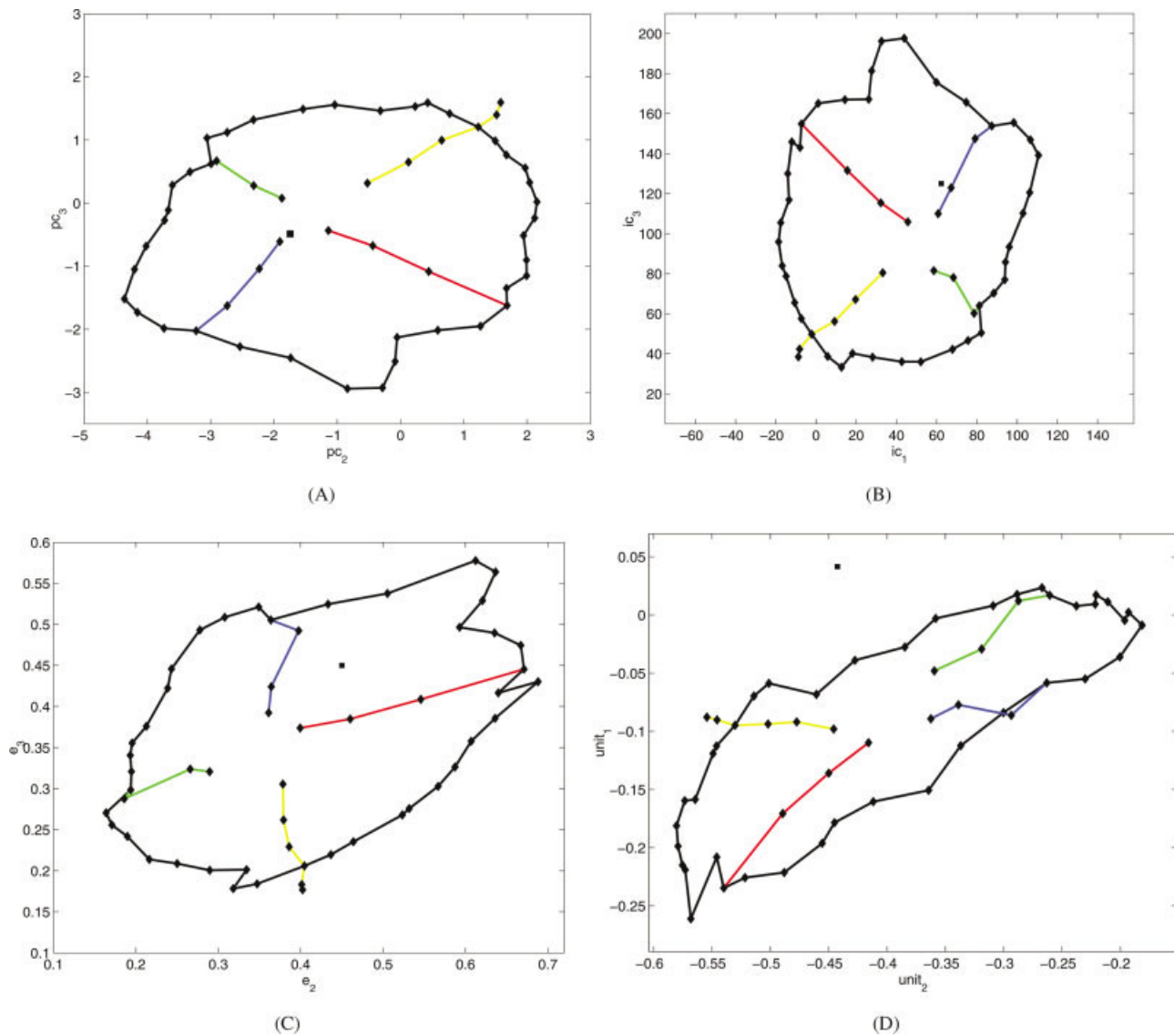


FIG. 4. 2D plots of the projections of samples belonging to the to value 7/ CCs. (A) PCA space, (B) ICA space, (C) NMF space, (D) neural network encodings. The spectral range is 380–800 nm.

certain hue sequences are not in ordinal order.) Many other arbitrarily selected sets of three continuous looped functions place the reflectances in ordinal order. PN and AP bases do not offer an advantage in this respect. In the sense of interval order these functions result in significantly less agreement with the psychological order than color-matching functions. This is shown by using an extract of the Munsell system previously called by one of the authors Celtic crosses (CC).<sup>20</sup> A CC consisting of all available hue samples at chroma 8 at value 7/ has been used. In addition, constant hue colors of varying chroma ranging from 2 (at two-step intervals) to the maximum existing for the given hue have been added for those hues that fall nearest to the diagram axes in a linear CIE tristimulus opponent color diagram (7.5RP, 5Y, 10G, 5PB). A synthesized value 7/ reflectance function was added to the two crosses. It is shown using a black square symbol. Notice the placement of the achromatic sample in each of the reconstructions.

For PCA, the first basis vector may be considered to

roughly describe the “lightness” axis (see Fig. 1A). The 2nd and 3rd eigenvectors roughly represent “red-green” and “yellow-blue” axes, respectively. In Fig. 4A the data are projected onto the plane spanned by the 2nd and 3rd most dominant eigenvectors. The normalized ICA bases are similar to the PCA bases; hence the same ideas are used for creating the “chromaticity” diagrams in Fig. 4B. Note, ICA can generate the ICs only up to a multiplicative sign; hence the sign change for the 2nd and 3rd ICs. Unlike PCA and ICA, the all-positive NMF bases seem to represent roughly “green”, “red” and “blue” filters, respectively (see Fig. 1D). The plot in Fig. 4C is a projection onto the plane spanned by the “red” and “blue” descriptors. For comparison, in Fig. 5A, B the CCs are also shown in the CIE X, Z diagram, respectively the CIELAB  $a^*$ ,  $b^*$  diagram. The superior reproduction in terms of intervals of the psychological diagram CC in the  $a^*$ ,  $b^*$  diagram compared to all spectral diagrams is evident. Calculations have also been made for a value 5 CC (not illustrated). The results are comparable.

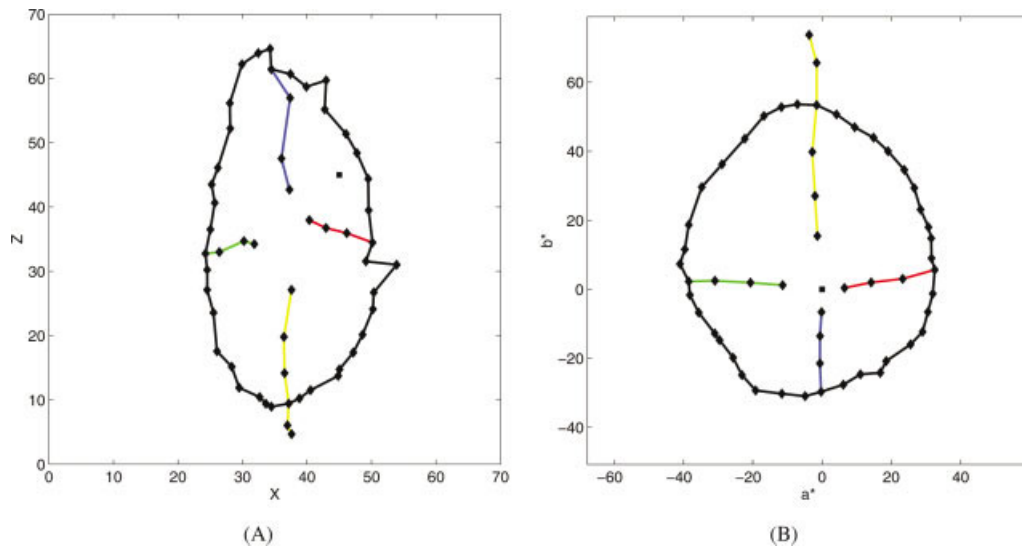


FIG. 5. 2D plots of the projections of samples belonging to the to value 7/ CCs in (A) CIE XYZ space, (B) CIELAB space.

### Lightness

In Figs. 4 and 5 the CCs are shown only in two dimensions. In the spectral spaces they are not located in a horizontal plane because none of the functions of those spaces is in agreement with the CIE luminosity function. This is illustrated in Fig. 6 for PCA. While in the CIE tristimulus space CCs fall on horizontal planes this is not the case for the spectral spaces. Romney and Indow who placed narrow range Joensuu reflectances into a PCA space introduced an average tilt so that constant value colors fall on an approximately horizontal plane.<sup>17</sup>

### Metamers

A particular aspect of color matching functions is that they place matching reflectances into the same location in

space. In spectral spaces this is no longer the case. Spectral spaces, therefore, cannot be in agreement with perceptual spaces as they imply different appearances for visual metamers and differences between these appearances where there are none. There are metamers specific to these functions that are different from perceptual metamers. They are located in different places in psychophysical color spaces.

Separation of psychophysical metamers in spectral spaces is demonstrated with the help of a large synthetic metamer each for the following Munsell colors at value 7/ and chroma 8: 5R, 5Y, 5G, 5B as well as an achromatic gray. Figure 7A illustrates the Joensuu reflectances and their metamers for the EE illuminant in the X, Z plane of the CIE tristimulus space. While the metamers are not perfect they are near-matches for the CIE 2° standard observer. Figure 7B-E show the same data in the PCA, ICA, NMF and NN diagrams. It is evident that the visual metameric pairs are represented in these diagrams in specific fashion, widely separated from each other.

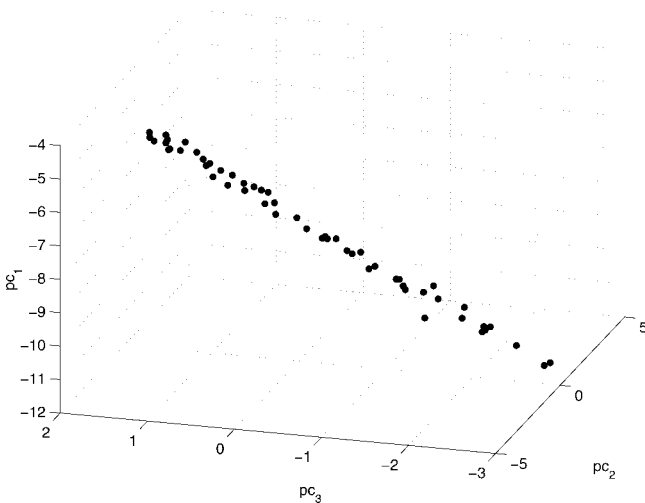


FIG. 6. 3D view of Munsell value 7/ CC, illustrating that neither do the samples lie in a plane nor are they in an arrangement parallel to the constituent planes for a PCA spectral space. The 3D view has been rotated such that this fact is best illustrated.

### INFORMATION EXTRACTION FROM REFLECTANCES BY THE VISUAL SYSTEM

Exact reconstruction of spectral functions does not appear to be a goal of the human visual system. More efficient reconstruction is possible with function shapes other than those of the cone response or color-matching functions. Evolution has chosen the particular cone functions (and the transformations of the opponent color system) perhaps from biological necessity. As a result the human visual system suffers from the drawback (or advantage) of a specific form of metamerism. It cannot distinguish between spectral returns that are metamers for the color matching functions. Such functions are distinguished with ease in spectral spaces (or by the visual system when the light source changes significantly). However, there is a reciprocal situation for metamers in spectral spaces.

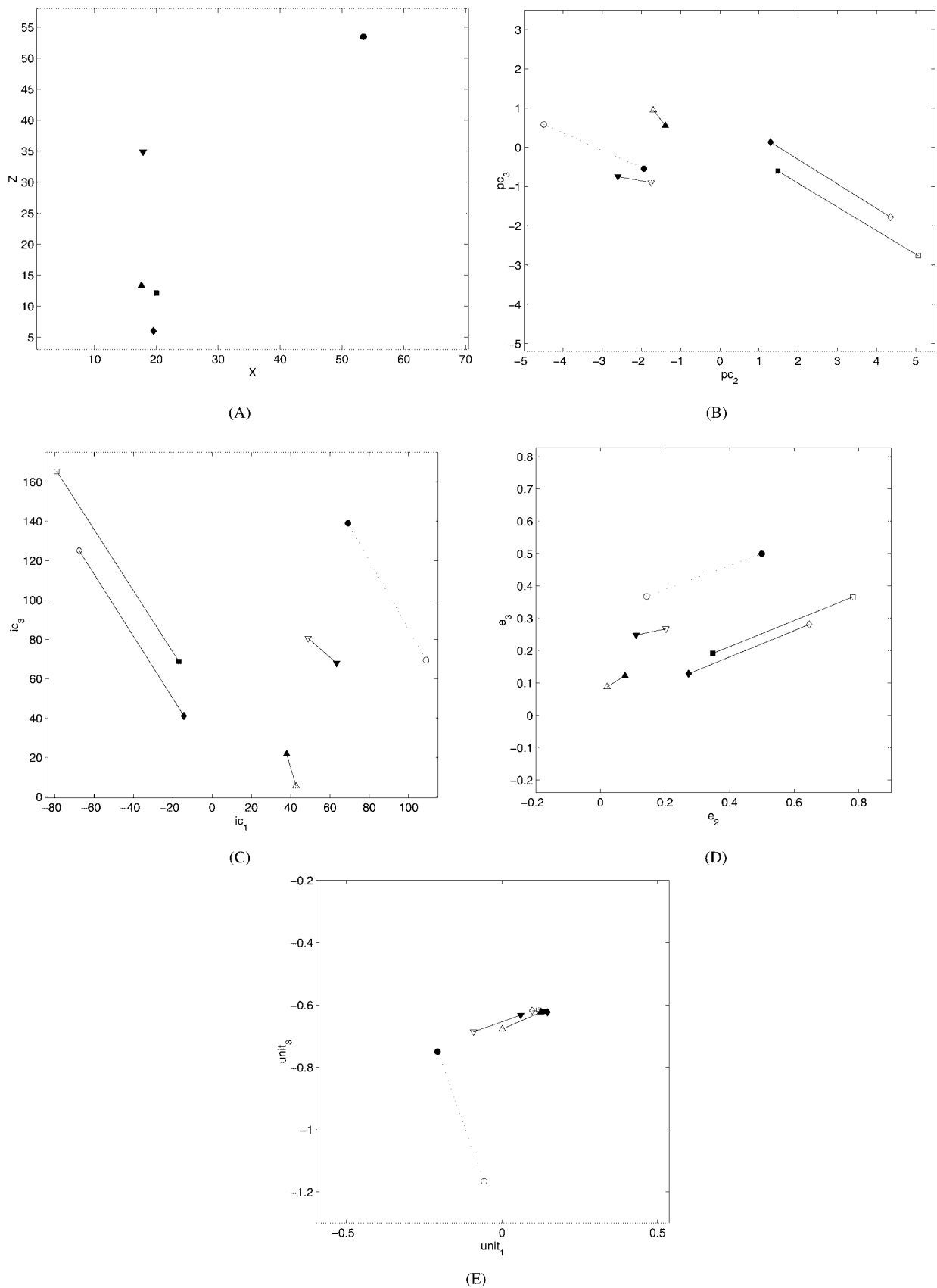


FIG. 7. 2D plots showing four chromatic samples (solid markers) and one achromatic sample and a synthetic metamer for each (empty markers) pairs in (A) XZ diagram, (B) PCA system, (C) ICA system, (D) NMF system, (E) NN system. Munsell samples used are 5R/8 (■), 5Y/8 (◆), 5G/8 (▲), 5B/8 (▼) and an achromatic sample (●). Metameric pairs are connected with lines. The pair associated with the achromatic sample is connected with the dashed line.

## CONCLUSIONS

Psychophysical uniform color spaces place samples representing (in a specific set of conditions) equal interval color scales into interval order that is in reasonable to good agreement with the perceptual interval order. Spectral spaces differ from interval level color spaces as follows:

1. They depend on the mathematical dimension reduction model used (see Fig. 1)
2. They vary with the specific set of input data.
3. While they often place (as do many other sets of three continuous functions) sample spectra into ordinal order with respect to the perceptual order the interval order is much inferior to that of a psychophysical uniform color space (see Fig. 4 A–D and Fig. 5B).
4. None of the axes of the spectral spaces is in agreement with perceived lightness (see Fig. 6 for an example)
5. They do not represent visual metamers in the same location. At the same time, samples that are metamers in a given spectral space are perceived by the average observer as different.

Spectral spaces are not color spaces. They lack specific relationship to human color vision and the term color space should not be used for them.

1. Cohen J. Dependency of the spectral reflectance curves of the Munsell color chips. *Psychonomic Sci* 1964;1:369–370.
2. Maloney LT, Wandell BA. Color constancy: A method for recovering surface spectral reflectance. *J Opt Soc Am A* 1986;3:29–33.
3. Maloney LT. Evaluation of linear models of surface spectral reflectance with small numbers of parameters. *J Opt Soc Am A* 1986;3:1673–1683.
4. Jaaskelainen T, Paarkkinen J, Toyooka S. Vector subspace model for color representation. *J Opt Soc Am A* 1990;7:725–730.
5. Lenz R, Osterberg M, Hiltunen J, Jaaskelainen T, Parkkinen J. Unsupervised filtering of color spectra. *J Opt Soc Am A* 1996;13:1315–1324.
6. Wachtler T, Lee TW, Sejnowski TJ. Chromatic structure of natural images. *J Opt Soc Am A* 2001;18:65–77.
7. Parkkinen JPS, Hallikainen J, Jaaskelainen T. Characteristic spectra of Munsell colors. *J Opt Soc Am A* 1989;6:318–322.
8. Vrhel MJ, Gershon R, Iwan LS. Measurement and analysis of object reflectance spectra. *Color Res Appl* 1994;19:4–9.
9. Maloney LT. Physics based approaches to modeling surface color perception. In: Gegenfurtner KR and Sharpe LT, editors. *Color vision, from genes to perception*. Cambridge: Cambridge University Press; 1999, 387–416.
10. Hyvärinen A, Oja E. Independent component analysis: Algorithms and applications. *Neural Networks* 2000;13:411–430.
11. Laamanen H, Jaaskelainen T, Parkkinen JPS. Comparison of PCA and ICA in color recognition. *Proceedings SPIE* 2001; 4197:367–377.
12. Usui S, Nakauchi S, Nakano M. Reconstruction of Munsell color space by a five-layer neural network. *J Opt Soc Am A* 1992;9:516–520.
13. Haykin S. *Neural Networks: A comprehensive foundation*. 2nd edition. New York: Prentice Hall; 1998.
14. Sharma G, Trussell HJ, Vrhel MJ. Optimal non-negative color scanning filters. *IEEE Trans Image Proc* 1998;7:129–133.
15. Lee DD, Seung HS. Learning the parts of objects by non-negative matrix factorization. *Nature* 1999;401:788–791.
16. Buchsbaum G, Bloch O. Color categories revealed by non-negative matrix factorization of Munsell color spectra. *Vision Res* 2002;42:559–563.
17. Lee DD, Seung HS. Algorithms for Non-negative Matrix Factorization. *Adv. Neural Info. Proc. Syst.* 2001;13:556–562.
18. Wyszecki G, Stiles WS. *Color science: concepts and methods, quantitative data and formulae*. 2nd edition. New York: Wiley, 1982, p 840–852.
19. Romney AK, Indow T. Munsell reflectance spectra represented in three-dimensional Euclidean space. *Color Res Appl* 2003;28:182–196.
20. Kuehni RG. Color space and its divisions. *Color Res Appl* 2001;26:209–222.